

Excited state charge transfer in covalently functionalized MoS₂ with zinc phthalocyanine donor-acceptor hybrid

Ruben Canton-Vitoria[#], Habtom B. Gobeze[#], Vicente M. Blas-Ferrando, Javier Ortiz, Youngwoo Jang, Fernando Fernández-Lázaro, Ángela Sastre-Santos, Yusuke Nakanishi, Hisanori Shinohara, Francis D' Souza,^{*} and Nikos Tagmatarchis^{*}

Abstract: Functionalization of MoS₂ is of paramount importance tailoring its properties towards optoelectronic applications and unlocking its full potential. Zinc phthalocyanine (ZnPc) carrying an 1,2-dithiolane oxide linker was employed to functionalize MoS₂ at defected sites located at the edges. The structure of ZnPc-MoS₂ was fully assessed by complementary spectroscopic, thermal and microscopy imaging techniques. An energy level diagram, to visualize different photochemical events in ZnPc-MoS₂ was established and revealed bi-directional electron transfer leading to ZnPc⁺-MoS₂⁻ charge separated state. Markedly, evidence of charge transfer in the hybrid was demonstrated using fluorescence spectroelectrochemistry. Systematic studies performed by femtosecond transient absorption revealed involvement of excitons generated in MoS₂ in promoting charge transfer, while such charge transfer was also possible when ZnPc was excited, signifying their potentiality in light energy harvesting devices.

Managing and controlling the electronic properties of semiconducting transition metal dichalcogenides (TMDs), which are governed by excitonic transitions, is mandatory for their realization in energy-related applications. To this end, among other sophisticated and complicated processes employed in nanosized semiconducting materials, a facile yet straightforward approach to gain precise control over the optoelectronic properties is by decorating the surface of TMDs with photo- and/or electro-active species and tuning charge-carrier density.^[1]

Phthalocyanines (Pcs) are robust electron rich systems with high capability to present charge separated states. Due to those competences and together with their great chemical stability, Pcs have been covalently connected with diverse

electron acceptors,^[2-8] and widely employed in photoinduced electron and/or energy transfer processes. Although only recently physisorption of Pcs on the basal plane of MoS₂ was reported,^[9, 10] covalent attachment on TMDs and evaluation of their photophysical behavior have yet to be performed.

The aim of the current work is to covalently incorporate zinc phthalocyanine (ZnPc) on MoS₂ and evaluate the efficiency of the newly derived hybrid material in photoinduced charge transfer (CT) reactions. The planar structure of the π -conjugated rings of ZnPc results in a flat-lying configuration over MoS₂, permitting efficient electronic interactions. To realize our aspirations, ZnPc carrying an 1,2-dithiolane oxide was prepared and employed to functionalize MoS₂. Using fluorescence spectroelectrochemistry, for the first time, direct evidence for the occurrence of CT in the hybrid was given. Additionally, the photophysical properties were evaluated via femtosecond transient absorption (fs-TA) spectroscopy and found that charge separation (CS) occurs, either by direct excitation of MoS₂ or ZnPc, leading to the formation of ZnPc⁺-MoS₂⁻ charge separated state.

The 1,2-dithiolane oxide modified ZnPc **1** (Figure 1) was prepared^[11] (Supporting Information, Figures S1, S2), and used in functionalizing exfoliated MoS₂. Reaction of **1** with MoS₂ afforded ZnPc-MoS₂ hybrid material **2** (Figure 1), according to our recently developed protocol with which 1,2-dithiolane derivatives add on S vacant sites at edges of MoS₂.^[12-14] The ZnPc-MoS₂ **2** was isolated via filtration of the reaction mixture on a PTFE membrane, followed by extensive washing with dichloromethane (Figure S3). The presence of *tert*-butyl units as side groups of ZnPc in **2** is beneficial for improving solubility (ca. 1.4 mg/mL in DMF) and stability in wet media (Figure S4), since they lay perpendicular to the Pc core, keeping apart adjacent MoS₂ layers via steric repulsive forces.

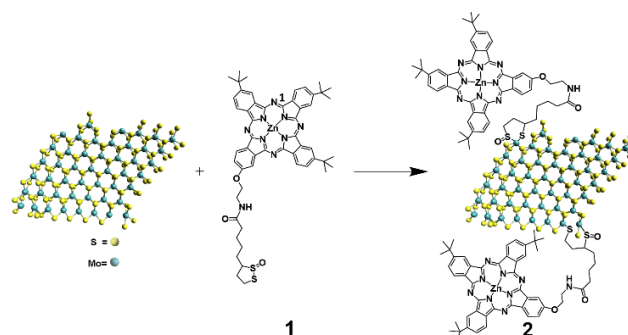


Figure 1. Functionalization of exfoliated semiconducting MoS₂ with ZnPc derivative **1** yielding ZnPc-MoS₂ **2**.

The Raman spectrum (λ_{exc} , 633 nm) of **2**, under on-resonance conditions for MoS₂, revealed not only characteristic modes for MoS₂ at 150-500 cm⁻¹ but also bands attributed to ZnPc at 1150-1600 cm⁻¹. Raman bands centered at 451, 403 and 379 cm⁻¹

[*] R. Canton-Vitoria, Prof. Dr. N. Tagmatarchis
Theoretical and Physical Chemistry Institute
National Hellenic Research Foundation
11635 Athens, Greece
E-mail: tagmatar@eie.gr

Dr. H. B. Gobeze, Y. Jang, Prof. Dr. F. D'Souza
Department of Chemistry
University of North Texas
305070 Denton, TX 76203-5017, USA.

Dr. V. M. Blas-Ferrando, Dr. J. Ortiz, Dr. F. Fernández-Lázaro,
Prof. Dr. Á. Sastre-Santos
Área de Química Orgánica, Instituto de Bioingeniería
Universidad Miguel Hernández
03202, Elche, Spain

Prof. Dr. N. Tagmatarchis, Prof. Dr. Y. Nakanishi, Prof. Dr. H.
Shinohara
Department of Chemistry
Nagoya University
Nagoya 464-8602, Japan

[#] These authors contributed equally.

Supporting information for this article is given via a link at the end of the document.

(Figure 2a) are associated to the 2LA(M) mode due to disorder and defects,^[15] the out-of-plane A_{1g} vibrations of S and the in-plane E_{12g} vibrations of S and Mo, respectively. The location of E_{12g} and A_{1g} , precisely their frequency difference calculated to be 24 cm^{-1} , is directly related with the thickness and number of layers of MoS_2 ,^[16] showcasing the presence of few MoS_2 layers in **2**. Markedly, the intensity ratio $2\text{LA(M)}/A_{1g}$ for **2** is found 0.5, decreased by around 60% as compared to the corresponding one for exfoliated MoS_2 , proving that the number of S vacancies was reduced. The latter is well understood by considering that MoS_2 functionalization occurred by grafting the 1,2-dithiolane moiety of **1** at edges possessing Mo atoms with S vacant sites. In addition, the A_{1g} and E_{12g} bands for **2** appear red-shifted by 2 cm^{-1} as compared with the ones due to exfoliated MoS_2 (ca. 401 and 377 cm^{-1} , respectively), attributed to intrahybrid CT phenomena between ZnPc and MoS_2 .^[17, 18] Specifically, the latter red-shift of these phonon modes is directly associated with n-doping of MoS_2 , as induced by electron donation from ZnPc within **2**. It is also worth noting the absence of the J_1 , J_2 and J_3 bands at 150 , 225 and 325 cm^{-1} , respectively,^[19, 20] attributed to the metallic MoS_2 polytype, therefore assuring that semiconducting is the predominant phase of MoS_2 in **2**. Focusing in the 1150 - 1600 cm^{-1} region (Figure 2a), ZnPc shows bands at 1214 and 1279 cm^{-1} related with the isoindole bending vibration, 1326 cm^{-1} due to C-C stretching vibration of pyrrole groups, 1424 cm^{-1} correlated with C-N-C bridging mode, while the most intense band is found at 1505 cm^{-1} corresponding to stretching vibration of C-C in the pyrrole ring.^[21]

The ATR-IR spectrum of **2** is mainly governed by the presence of aliphatic C-H stretching vibration bands at 2957 , 2916 and 2866 cm^{-1} , stretching and bending of the carbonyl amide and the C-N at 1652 and 1486 cm^{-1} (Figure 2b), respectively, corroborating the presence of ZnPc on MoS_2 .

Information related with the degree of functionalization and the loading of ZnPc in **2** was delivered by TGA. The thermal stability of **2** at 100 - $800\text{ }^\circ\text{C}$ under N_2 was assessed and compared with exfoliated MoS_2 and **1**. While exfoliated MoS_2 is thermally stable up to $500\text{ }^\circ\text{C}$ losing 2.9% up to $800\text{ }^\circ\text{C}$ due to presence of defects, **1** decomposes at 200 - $530\text{ }^\circ\text{C}$ leaving behind 50% due to Zn. For **2**, 2.1% mass loss observed at 200 - $550\text{ }^\circ\text{C}$ (Figure 2c) related with the presence of ZnPc covalently anchored on MoS_2 , representing one ZnPc per 103 MoS_2 units. The mass loss above $550\text{ }^\circ\text{C}$ is due to thermal decomposition of MoS_2 lattice at sites where initially ZnPc was anchored. Considering the covalent attachment of **1** at S-defect sites at edges of MoS_2 , the relatively low-loading of ZnPc was anticipated.

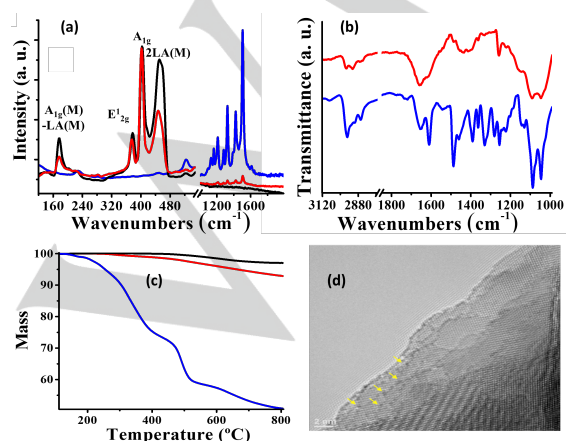


Figure 2. (a) Raman spectra normalized at the A_{1g} mode, (b) ATR-IR spectra, and (c) TGA graphs for exfoliated MoS_2 (black), ZnPc **1** (blue), and ZnPc- MoS_2 **2** (red). (d) Representative TEM image for **2**.

A typical HR-TEM image for **2** is shown in Figure 2d. After imaging numerous flakes, the lateral diameter of MoS_2 in exfoliated MoS_2 and hybrid material **2** is found to be around 100 nm on average. TEM imaging shows that dark dots, highlighted for clarity by yellow arrows, are localized at edges of MoS_2 , while the surface remains intact. In contrast to its surface, the edge of MoS_2 , at which S vacant sites are concentrated, are more reactive in the functionalization with the 1,2-dithiolane oxide moiety present in **1**. According to the aforementioned reactivity, the dark dots are attributed to Zn atoms of Pc.

Based on UV-Vis assays, **1** possesses characteristic absorption features, the Soret band at 348 nm and Q bands at 613 , 653 and 680 nm .^[22] In exfoliated MoS_2 , A and B excitonic transitions at 668 and 605 nm , respectively, followed by direct transitions from the valence to the conduction band at 456 and 374 nm (Figure S5) exist.^[23] Focusing in **2**, the major absorption due to ZnPc at around 680 nm masks the A excitonic band of MoS_2 , while in reverse the B excitonic band of MoS_2 overshadows the ZnPc absorption centered at 613 nm (Figure 3a). Although such overlapping effects do not allow to deliver robust and conclusive statements about possible electronic interactions between ZnPc and MoS_2 within hybrid **2** at the ground state, amelioration of the absorption of MoS_2 in the NIR region is evident.

Evaluating the electronic interactions at the excited states, upon excitation of **1** and **2** at 609 nm , for samples possessing same optical concentration, an appreciable quenching of ZnPc emission at 692 nm in **2** is observed (Figure 3b). The latter is in agreement with the corresponding fluorescence lifetime profiles (Figure 3c). While **1** exhibited typical monoexponential decay of 2.7 ns associated with the S_1 state, an additional three times faster lifetime decay was registered for **2**.

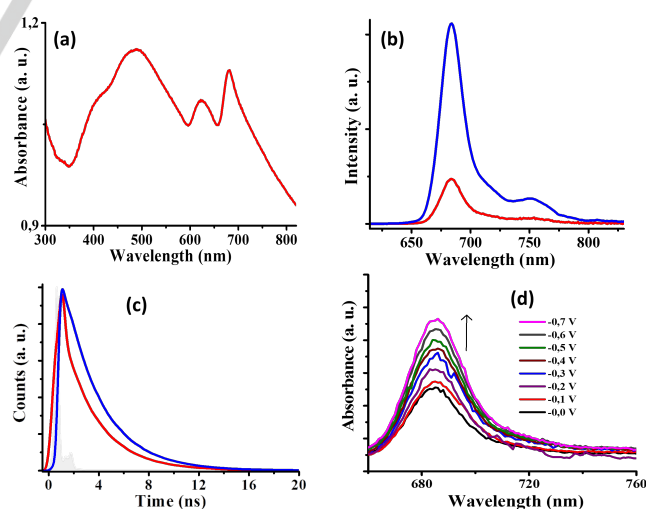


Figure 3. (a) UV-Vis spectrum for **2**. (b, c) Fluorescence spectra ($\lambda_{\text{exc}} 609\text{ nm}$) and decay profiles ($\lambda_{\text{exc}} 654\text{ nm}$) for **1** (blue) and **2** (red), respectively. (d) Fluorescence spectroelectrochemical changes for **2** ($\lambda_{\text{exc}} 650\text{ nm}$, with $0.2\text{ M n-Bu}_4\text{NClO}_4$ as electrolyte), revealing recovery of ZnPc emission upon reduction of MoS_2 . All spectral measurements were carried out in DMF.

Cyclic voltammograms of exfoliated MoS_2 , **1** and **2** in DMF vs Fc/Fc^+ are shown in Figure S6. Exfoliated MoS_2 revealed irreversible oxidations at -0.08 and 0.48 V and reductions at

-1.20 and -1.69 V.^[23, 24] The first oxidation and first reduction of **1** are located at 0.09 and -1.43 V. For **2**, overlapped and irreversible oxidation and reduction waves of MoS₂ and **1** were observed, broadening the voltammetric features. Nonetheless, both entities in **2** were found to be electroactive with facile oxidation potentials.

The electronic band structure of MoS₂ is thickness dependent.^[25, 26] Due to the strong hybridisation between the d-orbitals of Mo an indirect band-gap of around 1.23 eV exists, which is strongly dependent of the number of layers. Conversely, the direct band-gap of MoS₂ of around 1.89 eV is unaffected by interlayer interactions. The photoluminescence originating from the direct band-gap transition in MoS₂ (A exciton) is observed stronger and more intense by orders of magnitude in monolayer than in oligolayered and bulk material. Notably, although the photoluminescence energy due to the A exciton only slightly blue-shifts with decreasing thickness, the presence of large blue-shifts originating from the indirect band-gap transition, indicate strong and weak interlayer coupling for the indirect and direct transition, respectively.^[26, 27] In our work, the value of 1.12 eV for the band-gap of MoS₂ as derived from electrochemistry is close to the indirect band-gap value. Considering that the indirect band-gap of MoS₂ cannot be observed by electronic absorption and/or fluorescence spectroscopy, electrochemistry of few-layered MoS₂ seems to provide meaningful insight on its identification and assessment.

Support for occurrence of excited state CT leading to ZnPc^{•+}-MoS₂^{•-}, that is, ¹ZnPc* acting as an electron donor and MoS₂ as an acceptor, was arrived by fluorescence spectroelectrochemistry. If MoS₂ was electrochemically reduced, then the excited state CT from ¹ZnPc* would be diminished, restoring the quenched fluorescence of ZnPc in **2**. This is indeed found to be true, where an enhancement in fluorescence emission was observed when **2** was reduced (Figure 3d) at an applied voltage of -0.7 V vs Ag/AgCl corresponding to MoS₂ reduction and not that of ZnPc.

An energy level diagram was constructed to visualize the different photochemical events (Figure 4). The excited state energy $E_{0,0}$ for MoS₂ was found to be 1.83 eV (corresponding to the value due to the direct band-gap) compared to that of ¹ZnPc* being 1.80 eV, both determined from the corresponding midpoint of absorption and emission peaks. Regarding the energy alignment due to ground state interactions, considering these are minimal, they were not accounted in the energy level calculation. Due to low oxidation potentials of both MoS₂ and ZnPc, both entities were treated as electron donors to their counterparts from their respective excited states. Using the spectral and electrochemical results, the free-energy change for CS and charge recombination was estimated by employing the Rehm-Weller approach.^[28] Such calculations show that formation of ZnPc^{•+}-MoS₂^{•+} and ZnPc^{•+}-MoS₂^{•-} are both thermodynamically possible, either from the direct band-gap of MoS₂ or ¹ZnPc* excitation, however, the formation of ZnPc^{•+}-MoS₂^{•-} is more feasible by ~0.06 eV. Similarly, the energy level for ZnPc^{•+}-MoS₂^{•+} and ZnPc^{•+}-MoS₂^{•-} was calculated to be 1.35 and 1.29 eV, respectively. Additionally, the triplet ³ZnPc* level is higher than that of ZnPc^{•+}-MoS₂^{•-} CS state by 0.10 eV. Under such conditions ZnPc^{•+}-MoS₂^{•-} would charge recombine to ground state or populate ³ZnPc*. Singlet-singlet energy transfer from ¹ZnPc* to MoS₂ is an uphill process by 0.09 eV, however, this

process cannot be fully ruled out due to an almost isoenergy of the excited state of both entities and strong spectral overlap.

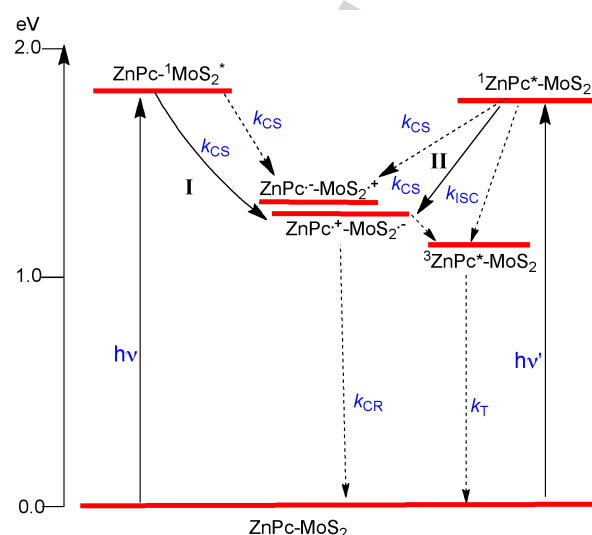


Figure 4. Energy level diagram showing possible photochemical events occurring in ZnPc-MoS₂ hybrid material **2**. Solid arrows show major processes while dashed arrows show minor ones.

Next, the effect of excited state CT on the photodynamics of **2** was investigated. Figures 5a-c and d-f show the fs-TA at selected delay times and species associated spectra (SAS) for exfoliated MoS₂ and ZnPc-MoS₂ hybrid **2**, respectively, excited at 425 nm corresponding to mainly the MoS₂. To analyze the transient spectral results, the recently proposed model by Guld^[23] based on detailed fs-TA studies of exfoliated MoS₂ in organic solvents was employed. To this end, the initial spectrum recorded for exfoliated MoS₂ at 1.6 ps revealed three minima at 502, 637, and 694 nm, and two maxima at 596 and 662 nm (Figure 5a). Throughout the first 10 ps, all of new features were subjected to blue-shifts possibly due to cooling of hot excitons^[32] and/or interexcitonic interactions.^[33, 34] The three bleaching fingerprints reflected the excitonic transitions seen in the steady-state absorption spectra.^[32] The kinetic profiles of the excitonic peaks revealed multiexponential fits making further deconvolution at this time scale difficult. Hence, a target-fitting program, Glotaran, was used for detailed kinetic evaluations^[33, 34] and generate SAS (Figure 5c). The rise and decay could be adequately fitted using five components, while the lifetimes of individual SAS were largely associated with their corresponding transient absorption spectra. The first component at 1.10 ps had three excitonic bleaching at 487, 631 and 691 nm corresponding to ground state absorption of excitons C, B, and A, respectively. The next two components at 5.56 and 151 ps, had growth of positive components. The formation of bi and/or multiexcitons and their decay could likely contribute to the 5.6 ps component in the growth and 151 ps in the decay, respectively. The next two components at 1.24 and 10 ns, had decay of the positive components, although the 10 ns was an overestimation as it exceeded the time resolution of our femtosecond setup. The 1.24 ns was earlier ascribed to photocharged state that interacts with the exciton generating triions.^[23]

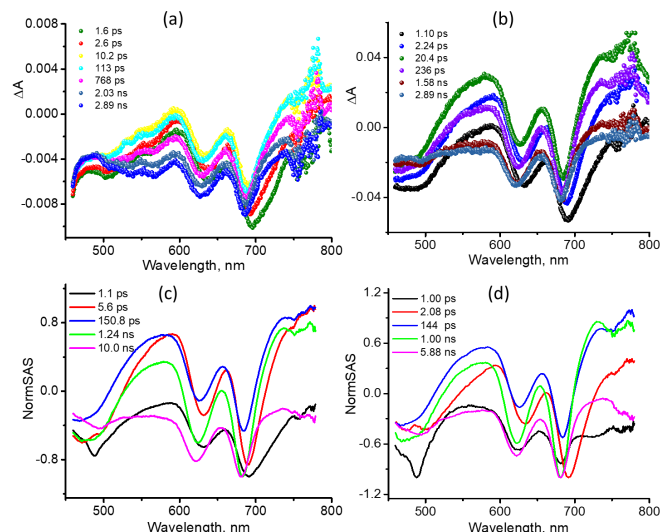


Figure 5. fs-TA spectra at the indicated delay times in DMF (λ_{exc} 425 nm), and normalized SAS derived from Glotaran analysis, respectively, for (a and c) exfoliated MoS₂, and (b and d) hybrid **2**.

The CS from excited MoS₂ to appended ZnPc depends on efficient formation of exciton, biexcitons and trions, dissociation of these species to free charge carriers, and transfer of charges to generate ZnPc⁺-MoS₂⁻ prior the occurrence of the recombination processes within MoS₂ (route I in Figure 4). In **2**, if CS occurs via the indirect band-gap from excited MoS₂ to ZnPc, then that would affect the lifetime of the transients, to be specific, could shorten the lifetime of these transients. The transient spectra of **2** were much better defined compared to exfoliated MoS₂ due to better solubility of the former. The growth and decay of excitonic peaks, as shown in the transient spectra, (Figure 5b) were noticeably different. Consequently, these data were subjected to Glotaran analysis^[33, 34] where five-component fit was satisfactory. That is, the first component being the beginning of excitonic peak formation, the next two being the exciton growth and the decay, and the last components being primarily due to the decay of positive components. Importantly, the time constants of each component were considerably shortened compared to the time constants of exfoliated MoS₂, meaning their involvement in CT to covalently linked ZnPc in **2**. However, the smaller change in the magnitude of these time constants suggests the CT interactions to be much weaker.

Next, the samples were excited at 370 nm, where both MoS₂ and ZnPc have absorbance. Figure S7 shows the SAS along with their time constants. The spectral features resembled close to that obtained when samples were excited at 425 nm. This was especially true for **2**, where peaks corresponding to ZnPc were missing, mainly due to their low availability compared to MoS₂ in the hybrid material. Importantly, faster time constants for **2** compared to exfoliated MoS₂ were observed, once again, ascertaining involvement of poly-excitons in the CS process.

Finally, both pristine ZnPc and **2** were excited at 675 nm, exciting mainly the ZnPc entity (Figure 6). For **2**, the transient spectra revealed negative signals at 620 and 675 nm due to ground state bleaching with some contributions of stimulated emission in the latter signal. In addition, a positive peak at 590 nm originating from transitions involving ¹ZnPc* was also observed. These signals lasted over 3 ns in agreement with the fluorescence lifetime of ZnPc being 3.14 ns. Interestingly, for **2**, decay of the positive peak and recovery of the negative ones

were much faster than that observed for ZnPc, e.g., contributions of positive peak at 498 nm and negative peak at 607 nm of ¹ZnPc* were seldom seen by 550 fs. The time profiles of 713 nm exciton peak of MoS₂ in pristine and hybrid material is shown in Figure 6c. Faster relaxation for the hybrid material was witnessed. In addition, the longer part of 728 nm of the hybrid revealed photobleach gain compared to pristine MoS₂ (Figure S8). These observation support the occurrence of CS in **2**. The radical cation species ZnPc⁺ is characterized by a NIR peak at 840 nm,^[22] supporting CS in **2** and leading to the formation of ZnPc⁺-MoS₂⁻ charge separated product. Therefore, transient spectra in the NIR region were also recorded (Figure 6d). Weak positive absorbance covering the 800-900 nm range were clearly seen, and by less than 500 ps the peak completely vanished. It may be pointed out that in this spectral range some contributions from ³ZnPc* were also present. This decay was not associated with the rise of the new peak in the 450-550 nm range corresponding to ³ZnPc*^[35] suggesting that the CS state may directly relax to the ground state instead of populating the triplet state or the triplet signals are too weak due to the low loading of ZnPc in the hybrid material.

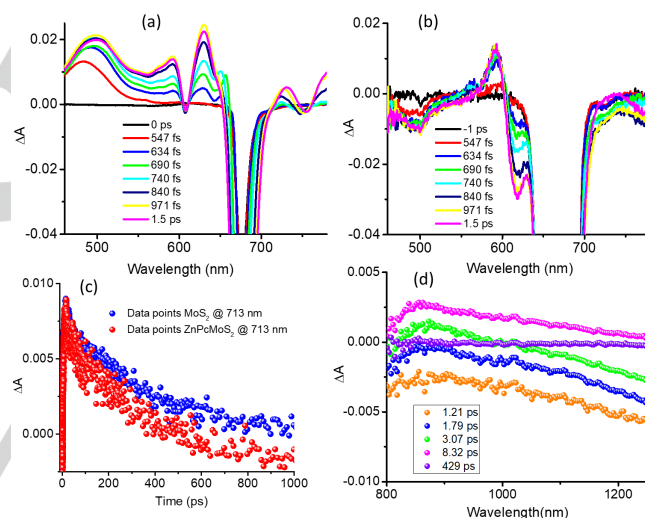


Figure 6. fs-TA spectra at the indicated delay times of (a) ZnPc **1**, and (b and d) ZnPc-MoS₂ hybrid **2** covering the visible and near-IR regions. (c) Decay profile of 713 nm peak of the indicated materials.

Earlier, electron transfer in thin films of non-covalently linked ZnPc/MoS₂ ensembles, formed via van der Waals interactions, were reported.^[9, 10] In one such study, involvement of the S₂ state and not that of S₁ of ZnPc in electron transfer was observed.^[9] The subtle differences in photochemical CT path are due to the nature of the sample, film vs solution, and the chemical functionalization modulating the energetics. In a similar study involving stacked ZnPc/MoS₂ in thin films, CS within 80 fs and recombination in 1-100 ps, was reported.^[36] The relatively slow CS and recombination in our system is consistent with the covalent bonding having a spacer linking the donor and acceptor entities within the hybrid material.

In summary, covalent grafting of ZnPc carrying an 1,2-dithiolane oxide linker on semiconducting MoS₂ was proven to be a versatile method of building ZnPc-MoS₂ donor-acceptor systems. By systematic optical absorption and fluorescence spectroscopy as well as redox studies, it was possible to construct an energy level diagram depicting different photochemical events which suggested bi-directional electron

transfer processes leading to $\text{ZnPc}^{+}\text{-MoS}_2^{-}$ charge separated product, either by direct band-gap excitation of MoS_2 or from $^1\text{ZnPc}^*$. Evidence for the occurrence of CT interactions in **2** was demonstrated by fluorescence spectroelectrochemistry, and this would form a key technique in future studies to demonstrate excited state CT in 2D nanomaterials. Further, systematic studies performed by fs-TA revealed the significance of different types of multi-excitons and their dissociation in promoting CT from $^1\text{MoS}^*$ to ZnPc . Additionally, direct excitation of ZnPc also promoted CS, where the charge separated state relaxed to the ground state instead of populating $^3\text{ZnPc}^*$. The present findings bring ZnPc-MoS_2 hybrids one step closer to build light energy harvesting devices.

Acknowledgments

Funding from EC H2020 research and innovation programme under Marie Skłodowska-Curie grant agreement N° 642742, the FY2018 JSPS Invitational Fellowship for Research in Japan (Long-term) ID N° L18520 to N.T., the Ministerio de Economía Industria y Competitividad of Spain (CTQ2014-55798-R and CTQ2017-87102-R) to A. S.-S. and UNT-AMMPI, US-NSF grant 1401188 to F.D. is acknowledged.

Keywords: transition metal dichalcogenides • phthalocyanines • functionalization • charge transfer • fluorescence spectroelectrochemistry

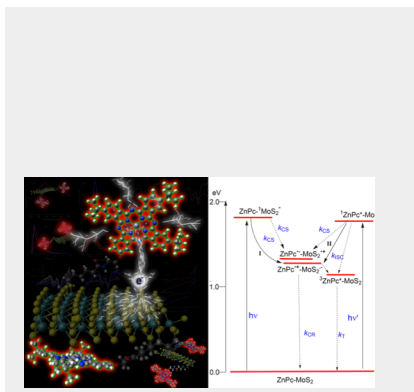
References

- [1] C. R. Ryder, J. D. Wood, S. A. Wells, M. C. Hersam, *ACS Nano* **2016**, *10*, 3900.
- [2] L. Martín-Gomis, F. Peralta-Ruiz, M. B. Thomas, F. Fernández-Lázaro, F. D'Souza, Á. Sastre-Santos, *Chem. Eur. J.* **2017**, *23*, 3863.
- [3] G. Rotas, L. Martín-Gomis, K. Ohkubo, F. Fernández-Lázaro, S. Fukuzumi, N. Tagmatarchis, Á. Sastre-Santos, *Chem. Eur. J.* **2016**, *22*, 15137.
- [4] L. M. Arellano, L. Martín-Gomis, H. B. Gobeze, M. Barrejón, D. Molina, M. J. Gómez-Escalonilla, J. L. G. Fierro, M. Zhang, M. Yudasaka, S. Iijima, F. D'Souza, F. Langa, Á. Sastre-Santos, *J. Mater. Chem. C* **2015**, *3*, 10215.
- [5] B. Ballesteros, G. de la Torre, C. Ehli, G. M. AA. Rahman, F. Agullo-Rueda, D. M. Guldi, T. Torres, *J. Am. Chem. Soc.* **2007**, *129*, 5061.
- [6] N. Karousis, J. Ortiz, K. Ohkubo, T. Hasobe, S. Fukuzumi, Á. Sastre-Santos, N. Tagmatarchis, *J. Phys. Chem. C* **2012**, *116*, 20564.
- [7] J. Malig, N. Jux, D. Kiessling, J.-J. Cid, P. Vázquez, T. Torres, D. M. Guldi, *Angew. Chem. Int. Ed.* **2011**, *50*, 3561.
- [8] V. M. Blas-Ferrando, J. Ortiz, V. González-Pedro, R. S. Sánchez, I. Mora-Seró, F. Fernández-Lázaro, Á. Sastre-Santos, *Adv. Funct. Mat.* **2015**, *25*, 3220.
- [9] E. P. Nguyen, B. J. Carey, C. J. Harrison, P. Atkin, K. J. Berean, E. Della Gaspera, J. Z. Ou, R. B. Kaner, K. Kalantar-zadeh, T. Daeneke, *Nanoscale* **2016**, *8*, 16276.
- [10] J. Choi, H. Zhang, J. H. Choi, *ACS Nano* **2016**, *10*, 1671.
- [11] H. G. Baldoví, V. M. Blas-Ferrando, J. Ortiz, H. Garcia, F. Fernández-Lázaro, Á. Sastre-Santos, *Chem. Phys. Chem.* **2016**, *17*, 1579.
- [12] R. Canton-Vitoria, Y. Sayed-Ahmad-Baraza, M. Pelaez-Fernandez, R. Arenal, C. Bittencourt, C. P. Ewels, N. Tagmatarchis, *NPJ 2D Mater. App.* **2017**, *1*, 13.
- [13] R. Canton-Vitoria, L. Vallan, E. Urriolabeitia, A. M. Benito, W. K. Maser, N. Tagmatarchis, *Chem. Eur. J.* **2018**, *24*, 10468.
- [14] R. Canton-Vitoria, C. Stangel, N. Tagmatarchis, *ACS Appl. Mater. Interfaces* **2018**, *10*, 23476.
- [15] S. Bae, N. Sugiyama, T. Matsuo, H. Raebiger, K.-i. Shudo, K. Ohno, *Phys. Rev. Appl.* **2017**, *7*, 024001.
- [16] H. Li, Q. Zhang, R. Y. C. Chong, K. T. Beng, T. E. T. Hang, A. Olivier, D. Baillargeat, *Adv. Funct. Mater.* **2012**, *22*, 1385.
- [17] B. Chakraborty, A. Bera, D. V. S. Muthu, S. Bhowmick, U. V. Waghmare, A. K. Sood, *Phys. Rev. B: Condens. Matter.* **2012**, *85*, 161403.

- [18] Y. Shi, K. Huang, L. Jin, Y. T. Hu, S. F. Yu, C. Li, L. Li, C. Yan, *Phys. Rev. B* **2013**, *87*, 085403.
- [19] S. J. Min, S. H. Cho, D. J. Wang, R. H. Friend, J. C. Lem, L. Li, C. Yan, *Phys. Rev. B* **2013**, *87*, 085403.
- [20] A. P. Nayak, T. Pandey, D. Voiry, J. Liu, S. T. Moran, A. Sharma, C. Tan, C. -H. Chen, L. -J. Li, M. Chhowalla, J. -F. Lin, A. K. Singh, D. Akinwande, *Nano Lett.* **2015**, *15*, 346.
- [21] C. Jennings, R. Aroca, A.-M. Hor, R.O. Loutfy, *J. Raman Spectrosc.* **1984**, *15*, 34.
- [22] S. K. Das, A. Mahler, A. K. Wilson, F. D'Souza, *ChemPhysChem*, **2014**, *15*, 2462.
- [23] L. Wibmer, S. Lages, T. Unruh, D. M. Guldi, *Adv. Mater.* **2018**, *30*, 1706702.
- [24] L. Vallan, R. Canton-Vitoria, H. B. Gobeze, Y. Jang, R. Arenal, A. M. Benito, W. K. Maser, F. D'Souza, N. Tagmatarchis, *J. Am. Chem. Soc.* **2018**, *140*, 13488.
- [25] W. S. Yun, S. W. Han, S. C. Hong, I. G. Kim, J. D. Lee, *Phys. Rev. B* **2012**, *85*, 033305.
- [26] K. F. Mak, C. Lee, J. Hone, J. Shan, T. F. Heinz, *Phys. Rev. Lett.* **2012**, *105*, 136805.
- [27] P. Tonndorf, R. Schmidt, P. Bottger, X. Zhang, J. Borner, A. Liebig, M. Albrecht, C. Kloc, O. Gordan, D. R. T. Zahn, S. M. De Vasconcellos, R. Bratschitsch, *Opt. Express* **2013**, *21*, 4908.
- [28] F. D'Souza, E. Maligaspe, K. Ohkubo, M. E. Zandler, N. K. Subbaiyan, S. Fukuzumi, *J. Am. Chem. Soc.* **2009**, *131*, 8787.
- [29] E. J. Sie, A. J. Frenzel, Y. H. Lee, J. Kong, N. Gedik, *Phys. Rev. B: Condens. Matter Mater. Phys.* **2015**, *92*, 1.
- [30] S. Sim, J. Park, J.-G. Song, C. In, Y.-S. Lee, H. Kim, H. Choi, *Phys. Rev. B* **2013**, *88*, 75434.
- [31] Z. Nie, R. Long, L. Sun, C. Huang, J. Zhang, *ACS Nano* **2014**, *8*, 10931.
- [32] T. Borzda, C. Gadermaier, N. Vujicic, P. Topolovsek, M. Borovsak, T. Mertelj, D. Viola, C. Manzoni, E. A. A. Pogna, D. Brida, M. R. Antognazza, F. Scotognella, G. Lanzani, G. Cerullo, D. Mihailovic, *Adv. Funct. Mater.* **2015**, *25*, 3351.
- [33] <http://glotaran.org/>
- [34] J. J. Snellenburg, S. P. Liptonok, R. Seger, K. M. Mullen, I. H. M. van Stokkum, *J. Stat. Software*, **2012**, *49*, 1.
- [35] R. Ashokkumar, A. Kathivaran, P. Ramamurthy, *Phys. Chem. Chem. Phys.* **2014**, *16*, 1015.
- [36] T. R. Kafle, B. Kattel, S. D. Lane, T. Wang, H. Zhao, W.-L. Chan, *ACS Nano*, **2017**, *11*, 10184.

COMMUNICATION

Covalent functionalization of two-dimensional semiconducting MoS₂ with an electron donating photosensitizer zinc phthalocyanine has been successfully achieved, and the hybrid material is shown to exhibit excited state charge transfer, pertinent towards optoelectronic applications.



R. Canton-Vitoria, H. B. Gobeze, V. M. Blas-Ferrando, J. Ortiz, Y. Jang, F. Fernández-Lázaro, Á. Sastre-Santos, Y. Nakanishi, H. Shinohara, F. D'Souza,* and N. Tagmatarchis*

Page No. – Page No.

Excited state charge transfer in covalently functionalized MoS₂ with zinc phthalocyanine donor-acceptor hybrid